

Propagation of Big Island eddies

Christina L. Holland and Gary T. Mitchum

College of Marine Science, University of South Florida, St. Petersburg, Florida

Abstract. Using satellite altimetry data, we have observed a series of anticyclonic eddies as they form at the Big Island of Hawaii and have tracked them as they move away from the island. While similar eddies have been observed near the Hawaiian Islands in previous studies, the fate of the anticyclonic eddies has previously been unclear. The eddies that we observed initially propagated to the southwest but consistently changed propagation direction to the northwest later in their lifetimes. This was intriguing to us, as theoretically, the decay of isolated anticyclonic eddies on a β plane should cause them to continually move toward the southwest. Such isolated eddy dynamics are unable to account for the observed change to northwestward eddy propagation, and the presence of the westward flowing North Equatorial Current turns out to be important to the Big Island eddy dynamics. The eddies are not passively advected by the North Equatorial Current; rather, the mean flow changes the propagation characteristics of the eddies. An existing theory that includes meridionally varying, purely zonal mean flow is shown to account for the observed propagation of the Big Island eddies if the zonal variation of the mean flow is considered.

1. Introduction

It has been known for some time [Patzert, 1969; Wyrki, 1982] that there is an active area of eddy generation in the lee of the Big Island of Hawaii. The eddy field is comprised of both cyclonic and anticyclonic eddy events, and several of these Hawaiian eddies were described in detail by Patzert [1969], although that study focused mainly on the cyclonic events. The cyclonic eddies moved away from the Big Island in a west/northwestward direction and essentially stayed near the Hawaiian Island chain throughout their lifetimes. There was a rather distinct boundary between the areas west of the Big Island that were dominated by cyclonic eddies (to the north) and by anticyclonic eddies (to the south). While the cyclonic eddies have been relatively well studied, the fate of the anticyclonic eddies after leaving the vicinity of the Big Island is unclear. Since mesoscale eddies carry both water mass and energy with them as they propagate, the speed and direction of their propagation as well as the length of their life could have important implications for the circulation and variability far away from their formation at the Hawaiian Islands.

It was just such a potential long-distance effect that initially prompted the present investigation into the propagation of these anticyclonic Big Island eddies. A series of episodic 90 day events was observed in the tide gauge sea level time series at Wake Island [Mitchum, 1995], which is located ~ 4200 km due west of the Big Island of Hawaii at $\sim 19^\circ\text{N}$, 165°E . It was shown that the 90-day signals at Wake Island were consistent with an energy source at the Hawaiian Ridge, and it was further hypothesized that the 90-day signals might be the remnants of the anticyclonic eddies generated at the Big Island. It was not known, however, if the eddies could persist and propagate from Hawaii to Wake Island and thus be responsible for the observations there. For this to occur, the net meridional propagation of the eddies would have to be essentially zero.

In addition to the eddy field, the Hawaiian Islands lie on the northern boundary of the equatorial current system and at the northern edge of the North Equatorial Current (NEC), specifically. The mean structure of the NEC was surveyed and described as part of the Hawaii-to-Tahiti shuttle experiment by Wyrki and Kilonsky [1984], who reported NEC flow between 9° and 18°N with an annual mean speed of 8.2 cm s^{-1} . We note as well that the NEC has strong seasonal variability, varying from $\sim 15\text{ cm s}^{-1}$ in the boreal fall to $\sim 5\text{ cm s}^{-1}$ in the boreal spring [Seckel, 1975]. In addition, the NEC is home to other mesoscale eddy variability, as described by Wyrki [1982]. Wyrki [1982] was most interested in a subset of the eddies that appeared to be formed within the NEC itself, at latitudes between 14° and 19°N . The NEC eddies were fairly frequent events, occurring in $\sim 50\%$ of the cruise sections across the NEC. These eddies moved ~ 10 km/day, which is similar to both the zonal speed of advection by the NEC and the baroclinic long Rossby wave propagation speed.

As will be described in section 2, we observed a consistently westward component of propagation for the anticyclonic Big Island eddies using TOPEX/Poseidon (T/P) altimetry data. Initially, the eddies moved to the southwest. Eddy dynamics on a β plane predict a southward component of propagation for anticyclonic eddies, as we will also discuss later. Of course, eddies propagating continually southwest from the Big Island of Hawaii could never reach Wake Island, as the two islands are at approximately the same latitude. When we tracked the eddies for longer periods of time, however, we were surprised to see them change direction. The early propagation was to the southwest, but somewhere between the longitudes of 170°E and 170°W , every one of the observed eddies stopped moving to the south. In fact, after reaching that critical region, they all began to propagate to the northwest. There was significant variation in detail between the individual eddy tracks, but this change in direction from southwestward to northwestward was a consistent feature of all of the eddy tracks (Figure 1).

This turn to northwestward propagation means that it might be possible for some of the Big Island eddies, or at least some

Copyright 2001 by the American Geophysical Union.

Paper number 2000JC000231.
0148-0227/01/2000JC000321\$09.00

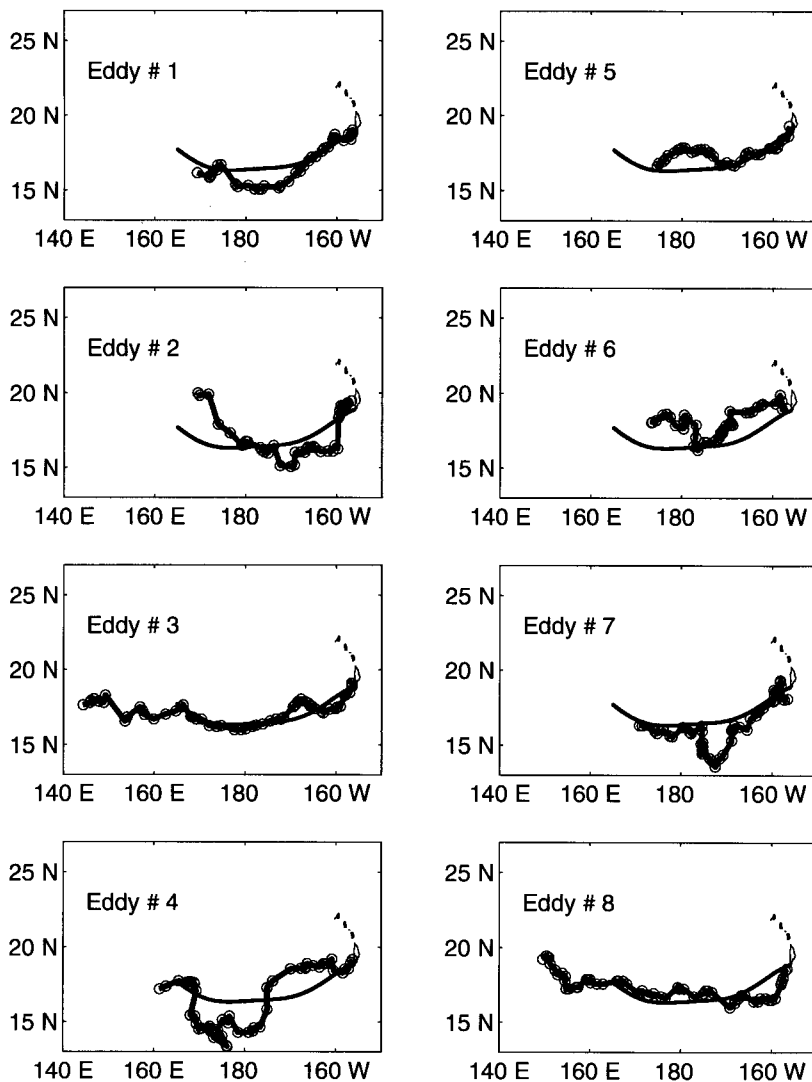


Figure 1. The observed tracks of the Big Island eddies. The positions of the eddies are plotted every 5 days from the time of their formation at the Big Island of Hawaii. The tracks were obtained using maps of gridded TOPEX/Poseidon altimetry data. Superimposed on the tracks is a composite eddy track, which was computed by averaging the eddy latitudes in 1° bins and smoothing by fitting a sum of sinusoidal functions to that curve by least squares.

residual signal associated with their decay, to have reached Wake Island. Only one of the eight observed eddies could be tracked to the vicinity of Wake Island. At this time, given the available data, we cannot determine whether or not the energy associated with the anticyclonic Big Island eddies might explain the sea level variability at Wake Island observed by *Mitchum* [1995]. This northwestward turn in the observed eddy trajectories does, however, introduce an entirely new puzzle. Dynamics for an isolated anticyclonic eddy (in the Northern Hemisphere) predict that on a β plane it should continue to move southwestward throughout its lifetime. The underlying cause of the change we observed in the eddy propagation direction is therefore an intriguing question.

Obviously, though, eddies in the real world are unlikely to exist in complete isolation, and there are other processes to consider. In this case, an important factor is likely to be interaction with the NEC. After the eddies form at the Big Island of Hawaii, they propagate southwestward and approach the west-

ward flowing NEC, and interaction with the mean current might affect the propagation behavior. We have chosen to simplify the problem, treating the eddies as if they were isolated except for the NEC, to explore the possibilities afforded by those dynamics. In this study, we will examine the dynamics of interaction with a mean current like the NEC to determine whether that can account for the change in the meridional component of the observed eddy propagation. In so doing, previous studies of interactions between vortices and various types of mean flows will be particularly useful and these studies are briefly reviewed below. Future work in this area should include other interesting possibilities, such as interactions between the anticyclonic eddies and the cyclonic eddies which also form at the Big Island.

Section 2 describes the observations and the analysis that led to the eddy tracks shown in Figure 1. Following that is a discussion of some of the dynamical studies relevant to the problem of eddy propagation in Section 3. Specifically, we will

discuss both the propagation of isolated eddies on a β plane and the possible effects of eddies interacting with a mean zonal current. Finally, we will present calculations from climatological data in an attempt to diagnose the dynamics behind the observed eddy propagation.

2. Observed Eddy Paths

The initial observations of the Big Island eddies by *Patzert* [1969] were made from hydrographic surveys, but such data are not available for tracking the eddies over long distances and times. The eddies, do, however, have readily observable sea surface height signatures and can therefore be observed at tide gauges or by satellite altimeters. The altimeters have an obvious advantage due to the global spatial and quasi-synoptic coverage provided by TOPEX/Poseidon (T/P) and other satellite altimeters. Thus T/P is the primary tool that we used to observe the eddies as they propagated away from the Big Island. There is a problem, though, in that the average distance between the T/P passes at 19°N is \sim 150 km, which is comparable to the size of the eddies, so that reconstructing the eddy signatures in time and space can be difficult. This problem can be partially overcome by using data from multiple altimeters, and we also used data from the European Space Agency's ERS-1 mission in the early phases of our work.

Visualization of the eddy propagation is achieved with gridded sea surface maps. Initially, altimetric data from T/P and ERS-1 were merged and gridded to form a series of 5-day sea surface height anomaly maps. While the ERS-1 data set has a longer repeat period, 35 days, than does the T/P data set, the spatial resolution is much better than that of T/P, so that the two complement one another. Using this blended data set, we were able to track individual eddies without difficulty, owing partly to the relatively large diameters and amplitudes associated with the Big Island eddies. We also made maps from the T/P data alone, and while the maps from only T/P data appeared rougher than those comprised of both T/P and ERS-1 data, the observed positions of the eddy tracks were insensitive to this difference. Also, regardless of whether we use T/P and ERS-1 or T/P alone, it is important to take care in gridding the data to be sure that the analyzed height field is not unduly distorted. Several different gridding methods were therefore used in this analysis, and we found that the positions of the eddy tracks were insensitive to the particular scheme used. Since T/P has a longer data record than ERS-1, the final gridded map series was made using only the T/P data, which enabled us to observe a larger total number of eddies.

In addition to testing the gridded sea surface height fields by evaluating the sensitivity of our results to which data was included (i.e., T/P and ERS-1 or T/P alone) and to what type of gridding algorithm was used, we also attempted to verify the eddy locations using independent data. First, satellite sea surface temperature from the advanced very high resolution radiometer (AVHRR) satellites was examined for independent confirmation of what the gridded T/P maps showed. The AVHRR data, unlike data from T/P and other microwave altimeters, are received in a wide swath beneath the satellite rather than along a narrow nadir track. These data can be displayed as a map without any artificial gridding, which makes it a useful data set with which to evaluate the gridded T/P maps. The usefulness of the AVHRR data are limited, though, by large data gaps whenever clouds were in the sky. For this reason, monthly composite maps of the AVHRR sea surface

temperature were used. There were still only a limited set of AVHRR maps for the relevant region and time period with enough data to be useful. The set of AVHRR maps was insufficient for tracking the eddies from AVHRR alone, but comparisons could be made between the AVHRR and T/P maps at a number of specific times. The mesoscale features in these monthly AVHRR maps were qualitatively similar to those in the T/P gridded maps. The eddies can be seen in the same location in each data set and are of the same approximate size.

As a second independent check, sea level data from the tide gauge at Johnston Island (16.7°N, 169.5°W) was examined in relation to the T/P gridded maps. Five of the observed eddies passed within 100 km of the Johnston Island station. Positive sea level anomalies, which correspond to anticyclonic features, of the correct amplitude are observed in the tide gauge time series at the times at which these eddies passed Johnston Island (Figure 2). Note that the seasonal variation has been removed from the sea level series in Figure 2 in order to emphasize the mesoscale events. Also note that there are clearly many other similar features in the Johnston record, but our main concern is that the tide gauge records the passage of the Big Island eddies at the same times as the T/P gridded fields do. The other events in the tide gauge record are also observed in the T/P maps (i.e., the time series correlate well), but these events are not of interest in the present context. Given the lack of sensitivity to the data used to make the maps and the corroborating evidence from the AVHRR and tide gauge data, we concluded that we could safely track the Big Island eddies from the gridded sea surface height maps.

Using these maps, we were able to track eight anticyclonic eddies from the Big Island. These eight eddies formed between November of 1992 and July of 1996, which implies an average rate of just over two eddies per year. Initially, all of the observed eddies moved off to the southwest from the Big Island of Hawaii, although the individual trajectories were rather varied. Later, all eight of the eddies turned to the northwest between the longitudes of 170°E and 170°W and continued to propagate northwestward from that point (Figure 1). It is natural to ask whether these eight eddies that we tracked were all that were formed or whether our sample might be biased in some fashion. To address this question, we note that *Patzert* [1969] used data from a number of cruises near the Hawaiian Islands between 1949 and 1967. Three cruises between September 1952 and August 1953 each observed a single anticyclonic eddy. Then between May 1965 and May 1967 a total of five anticyclonic eddies were observed out of measurements made by eight different cruises. The frequency of anticyclonic eddies at the Big Island of Hawaii appears from these data to be approximately two to three eddies per year. We are therefore reasonably confident that with the T/P gridded data we were able to observe all of the anticyclonic eddies that were formed during our study period.

3. Dynamics of Eddy Propagation

Several studies have discussed the effects of a β plane and nonlinearities on the zonal and meridional propagation of isolated eddies [*Flierl*, 1977; *McWilliams and Flierl*, 1979; *Flierl*, 1984; *McWilliams et al.*, 1986]. None of these studies considered the potential effect of any mean flow on the eddy propagation; they dealt instead with the behavior of isolated eddies. A study by *Chang and Philander* [1989] addresses this gap. These authors considered the propagation of packets of

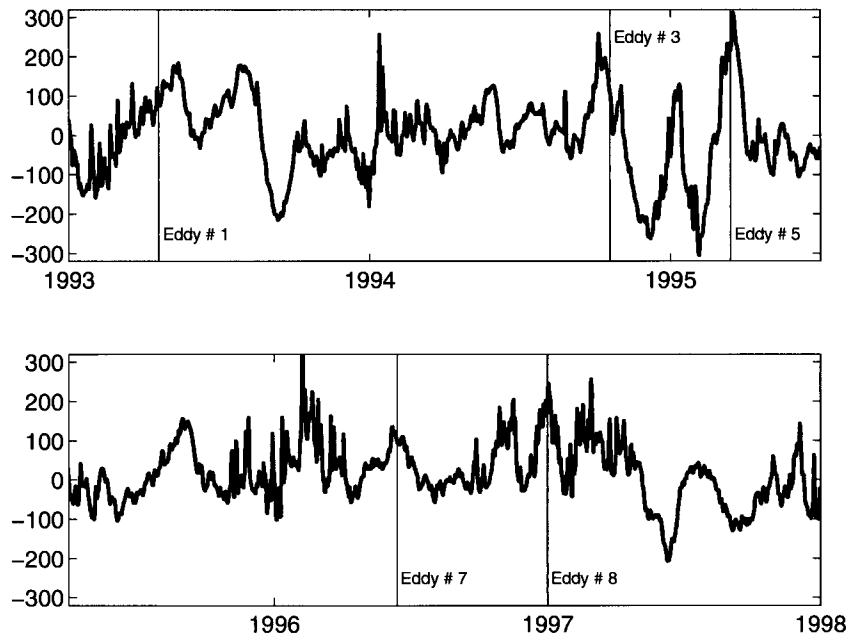


Figure 2. Five of the Big Island eddy events as seen in the time series of sea surface height taken from the tide gauge station at Johnston Island (16.7°N, 169.5°W). The best fit (in the least squares sense) of the annual cycle has been removed from the sea surface height time series. The times at which the eddies, as observed in the TOPEX/Poseidon gridded maps, most closely approached Johnston Island are shown as thin vertical lines.

Rossby waves in the presence of a mean, purely zonal, geostrophic current. Eddies can be viewed as a packet of Rossby waves, and the results of *Chang and Philander* [1989] are thus relevant to the case currently under consideration, that of an eddy approaching the NEC. We will first summarize the isolated eddy dynamics and then turn to the case of an eddy in a meridionally varying zonal mean flow.

3.1. An Isolated Eddy

An isolated eddy will propagate westward on a β plane, even under linear dynamics [*Flierl*, 1977]. In the study of *Flierl* [1977], mesoscale eddies are thought of as packets of Rossby waves, and as the individual Rossby wave components propagate westward, so does the complete eddy. The speed of the eddy's westward motion is simply the group speed of the Rossby waves making up the eddy. Initially the eddy is comprised of many different Rossby waves, and while all travel westward, their phase speeds are varied. Initially, then the westward propagation of the eddy is found to be at only $\sim 30\%$ of the long Rossby wave speed. This variety of propagation speeds in the wave components of the eddy causes the eddy to be dispersive and therefore to decay. As it propagates, it evolves, leaving behind a trail of slower Rossby waves. As those slower wave components are shed, the eddy amplitude decreases, and the westward propagation speed of the eddy increases toward the long Rossby wave speed. Everything discussed here thus far is true even for a linear eddy, but nonlinear effects can change the eddy evolution and propagation substantially. The nonlinear case, while it is a bit more complicated, is also more true to the real world of eddy propagation dynamics than the linear, so it is appropriate that we now address the effects of nonlinearity on the propagation of an isolated eddy. Nonlinear effects change the propagation behavior of anticyclonic eddies in two main ways [*McWilliams*

and *Flierl*, 1979; *Flierl*, 1984; *McWilliams et al.*, 1986; *Sutyrin and Flierl*, 1994]. First, the speed of westward propagation increases more rapidly than in the linear case and more closely approaches the expected long Rossby wave speed

$$c_x = -\beta\lambda^2, \quad (1)$$

in which λ is the Rossby radius of deformation written as

$$\lambda = (g'H/f_0^2)^{1/2}, \quad (2)$$

where g' and H are the reduced gravity and the upper layer thickness. Second, nonlinearity also induces a meridional component of propagation, through the development of a beta gyre [*Sutyrin and Flierl*, 1994]. The potential vorticity of the eddy

$$Q = (f + \zeta)/H, \quad (3)$$

where ζ is the relative vorticity, is conserved. The nonvortex part of the flow consists of the beta gyre, formed primarily by the advection of planetary vorticity and secondarily by distortions in the shape of the vortex. The meridional eddy propagation is controlled by the sign of the eddy's vorticity. An anticyclonic eddy propagates to the southwest under these dynamics in the absence of any mean flow. The maximum magnitude of the meridional propagation speed, for either cyclonic or anticyclonic eddies, is given by

$$|c_y| = (1/4)\beta\lambda^2 \quad (4)$$

[*McWilliams and Flierl*, 1979]. For cyclonic eddies, c_y is positive, while for anticyclonic eddies it is a negative quantity. Nothing about the dynamics of an isolated eddy, however, offers any explanation for anticyclonic eddies propagating to the northwest. If the eddies were only very weakly nonlinear, then their southward translation might be nearly nonexistent. Even if that were so, however, there is no reason in the theory

discussed up to this point for the eddies' meridional propagation to change direction as was observed. As discussed in section 1, though, the presence of the NEC probably cannot be ignored, so we will now consider mean flow effects on eddy propagation characteristics.

3.2. Effect of a Mean Current

Chang and Philander [1989] use essentially the same equations as the studies discussed above. Their model is nonlinear, on a β plane, and quasi-geostrophic for a single active layer above a lower layer assumed to be at rest. They use these dynamics to consider packets of Rossby waves interacting with a background mean flow. The mean flow U_0 is constrained to be geostrophic, purely zonal, and only variable meridionally; that is,

$$U_0 = U_0(y). \quad (5)$$

The existence of a mean current introduces a quantity B , which *Chang and Philander* term the "effective" β . The quantity B is defined as

$$B \equiv (f/Q)\partial Q/\partial y = [f/(f - \partial U_0/\partial y)] \cdot [\beta - (\partial^2 U_0/\partial y^2) - Q(\partial H_0/\partial y)], \quad (6)$$

where Q is the mean state potential vorticity,

$$Q \equiv [(f - \partial U_0/\partial y)/H_0], \quad (7)$$

which is dependent upon the planetary vorticity f , the mean relative vorticity $\partial U_0(y)/\partial y$, and the meridionally variable part of the mean thermocline depth $H_0(y)$. If the length scale L_0 over which the flow speed changes is large compared to the Rossby radius λ , (6) can be simplified. The term $f/[f - \partial U_0/\partial y]$ reduces to one, and the last term within the brackets in (6) is $Q(\partial H_0/\partial y)$, where Q , the potential vorticity, is approximately equal to f/H_0 . If the mean flow is assumed to be geostrophic, then this term can be approximated as

$$Q(\partial H_0/\partial y) \approx (f/H_0)\partial H_0/\partial y \approx -(f^2/g'H_0)U_0 \approx -U_0\lambda^{-2}, \quad (8)$$

where λ again represents the Rossby radius of deformation, so (6) becomes

$$B = \beta - \partial^2 U_0/\partial y^2 + \lambda^{-2}U_0. \quad (9)$$

The above discussion is in terms of packets of Rossby waves encountering a background current. It is more appropriate, however, to discuss nonlinear vortex dynamics in the context of the eddy-current interactions rather than simply treating the eddies as packets of Rossby waves. The following discussion starts from these nonlinear vortex dynamics [*McWilliams and Flierl*, 1979; *Sutyrin and Flierl*, 1994] and will show that the same effective β can be derived. Starting with the quasi-geostrophic equation for the streamfunction ψ ,

$$(\nabla^2 - \lambda^{-2})\partial\psi/\partial t + J(\psi, \nabla^2\psi) + \beta\partial\psi/\partial x = 0 \quad (10)$$

[*Sutyrin and Flierl*, 1994], where λ is the Rossby radius of deformation and J is the Jacobian, expressed as

$$J(\psi, \nabla^2\psi) \equiv (\partial\psi/\partial x)[\partial/\partial y(\nabla^2\psi)] - (\partial\psi/\partial y)[\partial/\partial x(\nabla^2\psi)], \quad (11)$$

it can easily be shown that the relative vorticity of the flow,

$$\Gamma = (\nabla^2 - \lambda^{-2})\psi, \quad (12)$$

obeys the relationship

$$D\Gamma/Dt = \partial\Gamma/\partial t + J(\psi, \Gamma) = -\beta\partial\psi/\partial x. \quad (13)$$

With the introduction of a zonal mean flow $U_0(y)$, such that

$$\partial\psi/\partial y = \partial\psi'/\partial y - U_0, \quad (14)$$

the vorticity equation becomes

$$D\Gamma'/Dt = \partial\Gamma'/\partial t + J(\psi, \Gamma') = -\beta'\partial\psi/\partial x, \quad (15)$$

$$\Gamma' = (\nabla^2 - \lambda^{-2})\psi' \quad (16)$$

$$\beta' = \beta - \partial^2 U_0/\partial y^2 + \lambda^{-2}U_0. \quad (17)$$

Expression (17) is identical to (9) for the effective β , B , from the *Chang and Philander* [1989] discussion for packets of Rossby waves. Expression (15) for conservation of potential vorticity for the anomalous flow (with respect to a mean flow) is identical to (13) for the no mean flow case, with the substitution of β' for β , so that the eddy propagation speeds (1) and (4) now become

$$c_x - U_0 = -\beta'\lambda^2 \quad (18)$$

$$c_y = -1/4\beta'\lambda^2 \quad (19)$$

for an anticyclonic eddy. Clearly, the speed and direction of propagation is dependent on the magnitude and sign of β' , the effective β . Understanding the meridional propagation of the Big Island eddies requires an understanding of the value of β' and how it changes throughout the lifetimes of the eddies. To that end, we will now consider some simplifications to (17), the expression for β' .

If L_0 is larger than λ , the shear of the mean flow is small and the second-term on the right-hand side of (9), $\partial^2 U_0/\partial y^2$, can be neglected. In most cases this is reasonable. At 10°N, for example, f is 2.5×10^{-5} , and if the internal gravity wave speed is taken as 2.7 m s^{-1} (a reasonable value but used here only for illustration), then the Rossby radius of deformation is 107 km, or just under 1° of latitude. The width of the mean flow, on the other hand, is usually several degrees. Except in regions of highest mean flow shear, the second term can be neglected, and β' can be approximated as

$$\beta' \approx \beta + U_0\lambda^{-2}. \quad (20)$$

Recall from (19) that the meridional speed is directly proportional to β' . If the mean flow is eastward, then the β' is larger than β , and the meridional propagation speed is increased. If an eddy were approaching such an eastward current from a region of slower or nonexistent mean flow, then this increase in meridional propagation would serve to carry it further into the current, thus increasing the mean flow it feels even more and so on. On the other hand, if the mean flow is westward like NEC, β' is less than β , and the meridional propagation speed is therefore decreased and eventually goes to zero at the latitude where $\beta' = 0$. The degree to which the meridional propagation is slowed depends mainly on the strength of the currents, except as noted earlier in regions of very strong meridional shear in the mean flow.

The expression for the zonal propagation speed (18) has two terms, one equal to the mean flow and one analogous to the long Rossby wave speed at which it propagates in the no mean flow case. The second term, like the expression for the meridional propagation speed, is directly proportional to β' rather than β , as it would be in the no mean flow case. As the strength

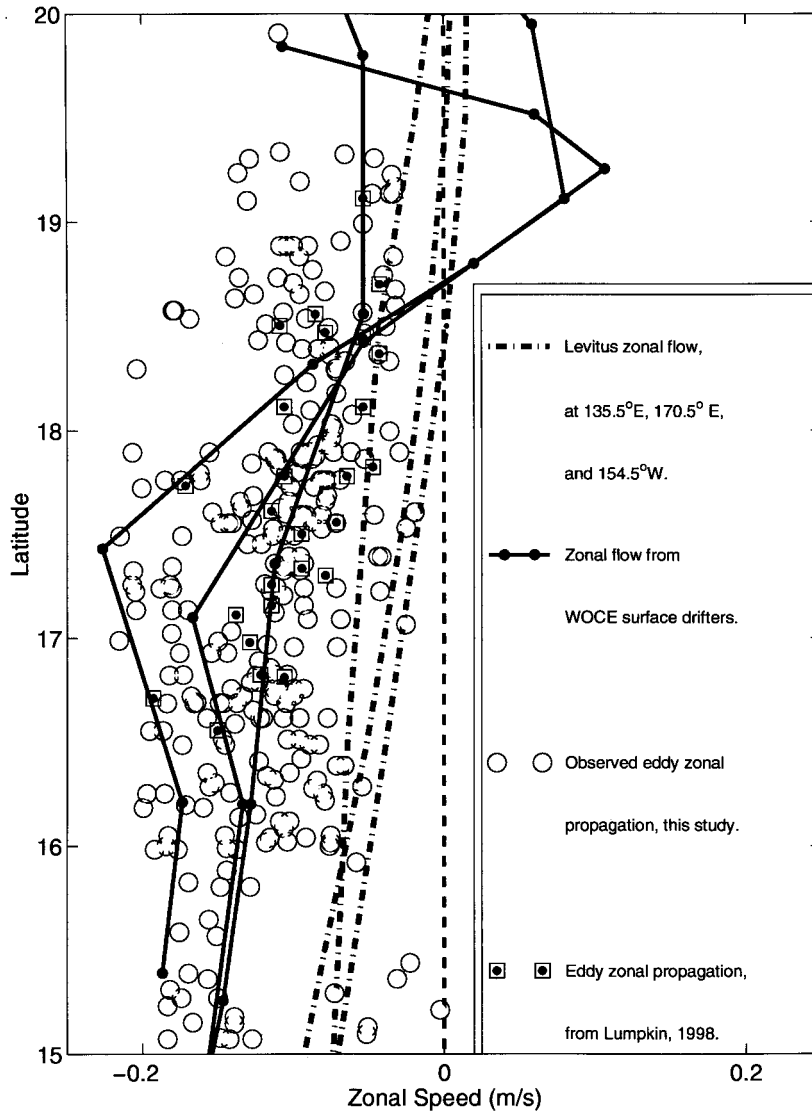


Figure 3. The zonal speed of the eddies, computed from the observed trajectories with a time step of 2 months. Also shown are the zonal eddy speeds computed by Lumpkin [1998], the Levitus *et al.* [1994] geostrophic U_0 , and the mean zonal speeds of the World Ocean Circulation Experiment (WOCE) surface drifters between 156.5° and 160° W, between 160° and 168° W, and between 170° and 180° W [Lumpkin, 1998].

of the westward mean flow that the eddy encounters increases, the value of the parameter β' decreases, and as this happens, the zonal propagation speed approaches the limit of

$$c_x = U_0 \quad (21)$$

at the same latitude where the meridional propagation component goes to zero. In a westward mean flow, it is therefore possible for the eddy paths to asymptote toward a critical latitude, which is simply the latitude where $\beta' = 0$. After reaching this point, the zonal propagation continues at a constant rate equal to the mean flow speed at that latitude. The meridional speed is zero, and so the eddies are unable to leave that critical latitude. If the eddy is thought of as a packet of Rossby waves as described by Chang and Philander [1989], all of the Rossby wave components of a packet of waves such as a mesoscale eddy would then be traveling at the same speed, that of the mean current at the critical latitude. The zonal propagation speeds of the anticyclonic eddies observed in this study

are faster than the geostrophic U_0 computed from the Levitus *et al.* [1994] climatological dynamic heights owing to the smooth nature of the climatology. As can be seen in Figure 3, however, the eddy propagation speeds do agree well with the World Ocean Circulation Experiment (WOCE) surface drifter derived zonal speeds [Lumpkin, 1998]. Chang and Philander [1989] suggest that the Rossby waves should be absorbed into the mean flow at the critical latitude as they cannot propagate away from it. In our observations, however, the eddies continue to be visible as distinct features in the sea surface height anomaly fields.

As discussed earlier, the Big Island eddies propagate to the southwest initially. Later, the southward component of their motion decreases, comes to a halt, and in fact, reverses, so that these anticyclonic eddies propagate to the northwest. On the basis of the above theory, interaction with a strong westward mean current such as the NEC seems to be a likely cause for this halting of the southward motion, but the northwestward

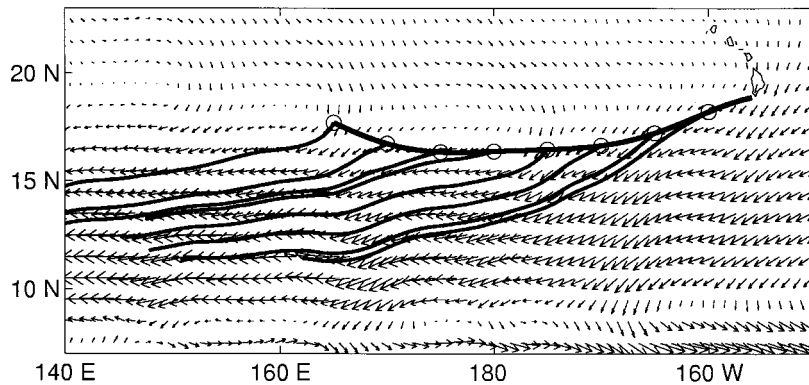


Figure 4. The composite eddy track compared to virtual drifter trajectories. The vector field is the surface geostrophic flow computed from the climatological [Levitus *et al.*, 1994] dynamic height relative to 1000 m. The thickest line is the composite eddy track, as in Figure 1. Virtual drifters were inserted into the climatological surface geostrophic flow at several locations along the composite eddy tracks. The daily positions of these virtual drifters, as inferred by the climatological flow, are shown.

propagation that follows that will require additional consideration.

3.3. Advection by the North Equatorial Current

The effective β from Sutyris and Flierl [1994] and Chang and Philander [1989] appears to offer a possible explanation for at least some of the observed propagation characteristics of the Big Island eddies, and later we will address the effect of a more complicated mean flow that is allowed to vary zonally in size and strength. First, though, it is natural to wonder whether there might be another, simpler way to account for the observed propagation. One possibility is that the eddies do not actively propagate at all but are simply advected passively to the northwest by the mean flow. We will therefore digress briefly to determine whether the eddy propagation might instead be accounted for by a simple advection processes.

From Section 3.2 [Chang and Philander, 1989; Sutyris and Flierl, 1994] we know that for the case where U_0 , H_0 , and β' are all functions of latitude only, the eddy propagation speeds at the point where β' approaches zero can be written as

$$c_x = U_0 \quad c_y = 0. \quad (22)$$

In this scenario, the eddy can be thought of as nondispersive and freely propagating at exactly the mean flow speed. Conversely, it could be imagined that the eddy is not freely propagating at all but rather is simply being advected along by the mean current after the point when it reaches the critical latitude. If the mean flow is a function of latitude only, it is impossible to test which of these views is correct. If, on the other hand, the mean flow U_0 varies with both latitude and longitude, then these two hypotheses can be easily tested against one another. All eight of the eddies observed in this study were incorporated into a composite eddy track (Figure 1) in order to more easily compare the eddy propagation to the mean flow. The mean flow used is the geostrophic flow at the surface, relative to the 1000 m depth level, computed from the Levitus *et al.* [1994] climatology.

We inserted virtual drifters into this mean field at several locations along the composite eddy track and plotted the drifter locations every day (Figure 4). If one supposes that the eddies, in moving northwestward, were simply advected by the mean flow of the NEC, then the virtual drifter trajectories

should also turn to the northwest. Those trajectories should, in fact, lie alongside the eddy path, but this does not appear to be true for any part of the eddies' lifetime. Instead, the climatological drifters move consistently to the southwest even after the eddy path has turned to the northwest. This does not eliminate the possibility that instantaneous variations in the NEC could advect eddies to the northwest, but for this to be a reasonable explanation for the very consistent northwestward turn of all of the observed eddies, we would expect to see some indication of northwest flow in the climatological current. Simple advection processes appear to be unable to account for the northwestward eddy motion, and so we now return to β' , the effective β , and discuss the case where the zonal flow is allowed to vary with longitude.

3.4. Zonal Variation in the Mean Flow

To attempt to explain why an anticyclonic eddy might move northwestward, we want to take the ideas of Sutyris and Flierl [1994] and Chang and Philander [1989] a step further. That is, can these dynamics, when extended to a mean flow that is neither purely zonal nor varying solely in the meridional direction, account for the observed change in the eddy propagation direction? Zonal variation in the mean flow alters β' , the effective β parameter, and therefore can further affect the propagation of mesoscale eddies. The NEC does in fact have spatial variability, with zonal variations in the flow speeds and in the latitude of the strongest flow (Figure 5). The speeds shown are the geostrophic speeds at the surface relative to 1000 m, again computed from the Levitus *et al.* [1994] climatological dynamic height data.

Recall that Sutyris and Flierl [1994] and Chang and Philander [1989] deal only with a purely zonal and purely meridionally varying flow $U_0(y)$, which is in geostrophic balance with the meridionally varying interface depth $H_0(y)$. Exposed to such a mean flow, the meridional motion of anticyclonic eddy depends on the effective β parameter, β' , which was shown above to be approximately

$$\beta'(y) = \beta - Q(y)\partial H_0(y)/\partial y. \quad (23)$$

The latitude at which $\beta' = 0$ was of particular interest, as that defined the expected path of the eddies in the presence of the mean flow. A more realistic case to consider is a current that

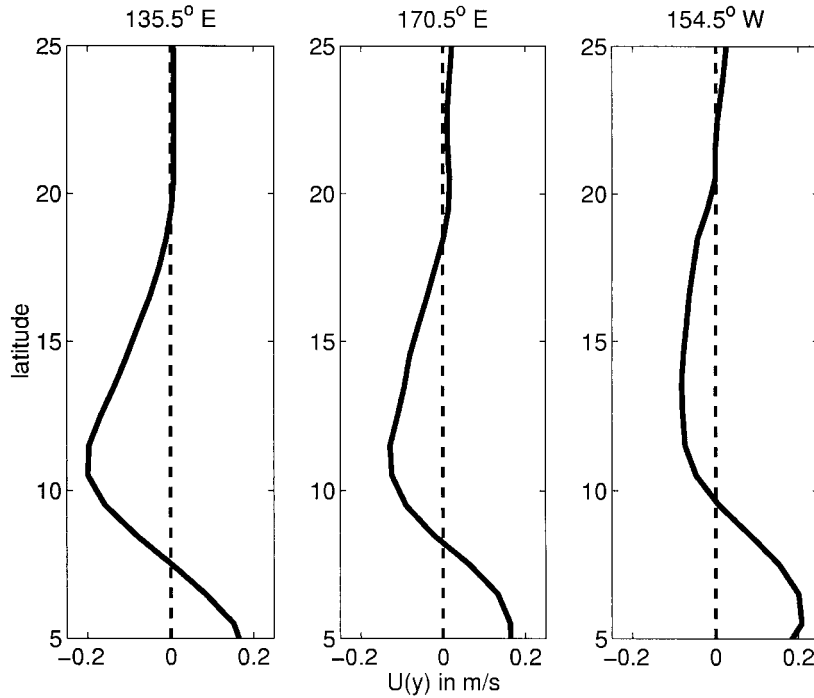


Figure 5. Zonal variation in the surface geostrophic flow of the NEC computed from the *Levitus et al.* [1994] climatological dynamic height relative to 1000 m. The x axis of each panel is the strength of the zonal component of the mean flow $U_0(y)$ (in m s^{-1}). The y axis in every case is latitude. The panels show the mean flow at (left) 135.5°E , (middle) 170.5°E , and (right) 154.5°W .

can vary in strength and width with longitude. The NEC, for instance, widens and strengthens as it moves westward. In this case, the latitude at which β' is approximately zero is no longer constant but rather varies with longitude; that is, there is a curve $y(x)$ defined by

$$\beta'[x, y(x)] = 0. \quad (24)$$

By analogy with the simpler $\beta'(y)$ case, we expect that if $y(x)$ is slowly changing zonally, then the eddy placed in such a mean flow field should follow the $\beta' = 0$ contour, once reaching it, for the remainder of its lifetime. The NEC has both zonal and meridional flow, but it is still primarily a zonal current, as can be seen in a vector map of geostrophic flow relative to 1000 m, computed from the *Levitus et al.* [1994] climatology (Figure 4). This greatly simplifies matters; if the NEC were not primarily a zonal current, the dispersion relation would differ from the form discussed earlier and would be much more complicated. As it stands, contours of β' and thus the expected path $y(x)$ can be estimated from the *Levitus et al.* [1994] climatology.

In order to make this estimate, we recall that the mean flow potential vorticity Q is approximately f/H_0 . This allows us to write (23) as

$$\beta' \approx \beta - (f/H_0)\partial H_0/\partial y, \quad (25)$$

which is a more convenient form since it only involves the interface depth. This quantity can be estimated from the *Levitus et al.* [1994] climatology. We could have inferred H_0 from the dynamic height relative to 1000 m from *Levitus et al.* [1994]. A better choice, however, is to use the actual depth of the pycnocline or at least the best estimate of that depth possible from the climatological data. The climatological values of temperature and salinity from *Levitus et al.* [1994] were used to

compute σ_θ profiles versus depth at each latitude and longitude. Inspection of these profiles suggested that σ_θ values of between 26.0 and 26.2 kg m^{-3} serve as a reasonable definition of the pycnocline in our study area, and the depth of these isopycnals are therefore used to define $H_0(y)$ at each grid point in the *Levitus et al.* [1994] climatology. These $H_0(y)$ can then be meridionally differentiated at each zonal position to obtain estimates of β' at each grid point. In determining the positions at each longitude where $\beta' = 0$, which define the $y(x)$ curve that we need, we first identified the region where β' decreases from 2 to $0 \times 10^{-12} \text{ m}^{-1} \text{ s}^{-1}$ as we approach the core of the NEC from the north. These regions are shown on Figure 6 for two calculations: one uses $\sigma_\theta = 26.0 \text{ kg m}^{-3}$ and the other uses $\sigma_\theta = 26.2 \text{ kg m}^{-3}$ as the definition of the pycnocline. There can, of course, be zero contours of B on both the north and south flanks of the NEC, but since the eddies are approaching the NEC from the north side, only the contours of β' on the north side of the core of the NEC are shown because these are considered to be the dynamically important ones.

For comparison, the composite of the observed eddy tracks is also included on Figure 6, and the close correspondence between the average eddy path and the $y(x)$ estimates supports the idea that the basic *Sutyrin and Flierl* [1994] and *Chang and Philander* [1989] theory can account for the general propagation characteristics of the Big Island eddies. In fact, it appears from this analysis that the Big Island eddies are never truly isolated; they are formed in close proximity to the $\beta' = 0$ contour and remain with it throughout their lifetimes. It does not appear to be necessary to invoke β plane dynamics for an isolated eddy at all to explain the zonal propagation in this case. The zonal propagation is controlled, along the zero β' contour, by the mean zonal flow component. The meridional

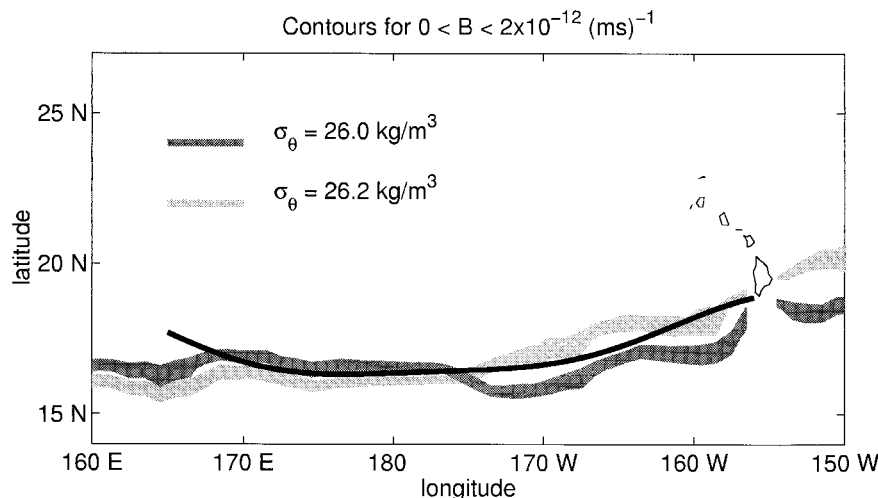


Figure 6. The composite eddy track compared to the zero contour of B , the effective β of *Chang and Philander* [1989]. β' is computed from the *Levitus et al.* [1994] climatology of temperature and salinity according to $\beta' = \beta - (f/H_0)\partial H_0/\partial y$, where H_0 is the thermocline depth, estimated from the depths of σ_θ contours. The solid line is the composite eddy track, and the medium and light shaded lines curves are the zero contours of B on the north side of the north equatorial current based on the depths of σ_θ equal to 26.0 and 26.2 kg m^{-3} , respectively.

propagation, on the other hand, depends on the zonally variable position of the gradient of the Coriolis parameter and of the position, strength, and latitudinal shear of the background mean current. From the point of their formation at the Big Island of Hawaii the eddies appear to remain on the zero contour of β' through much, if not most, of their lifetimes.

4. Future Work

The propagation of the anticyclonic Big Island eddies can be explained by their following the $\beta' = 0$ contour, where β' is the effective β . This effective β differs from the planetary β owing to the presence of a mean background current, the NEC. This is, of course, not the only possible explanation, and further research is needed. One topic requiring further study is the stability of the NEC. It is possible that for a large-scale current, such as the NEC, if it is stable, the meridional gradient of potential vorticity and the advection effects balance, producing only small net effects on vortex propagation. Since we found that β' has a zero contour, though, the NEC may be an unstable current. In fact, the Charney-Stern condition for instability of a flow is that the meridional gradient of the potential vorticity, which has been designated here as β' , must change sign somewhere within the flow [*Charney and Stern*, 1962]. This is a necessary but not a sufficient condition of instability, so we cannot say from this alone whether or not the NEC is unstable. The question of the stability or instability of the NEC could have important consequences when eddy-current interactions and subsequent eddy propagation are considered. The data for the mean NEC available at the time of this study [*Levitus et al.*, 1994] are not sufficient owing, in particular, to their heavily smoothed nature to determine whether the NEC is stable or unstable. Better climatological data sets, such as the recently released World Ocean Database [*Levitus et al.*, 1998] may allow this question to be answered. Another approach to the problem would be to examine the sea surface height expression of the eddies in detail as they propagate and evolve. The evolution of the structure of the eddies would provide further

insight into the nature of the eddy-current interactions and the stability of the mean current. The altimetric data used in this study, while sufficient for determining the position of the eddies as they propagate, will not allow such detailed plots of the eddy structure as would be required for this purpose owing to the cross-track resolution of the altimeter and the difficulty of separating the eddies from the surrounding variability. New data products, such as the recent high-resolution mapping using combinations of T/P, ERS-1, and ERS-2 [*Ducet et al.*, 2000], may make this a practical approach.

Another interesting area for future work is the possibility of interactions between individual eddies. In this study, we have focused exclusively on the effect of the NEC on the eddy propagation, treating these anticyclonic eddies as if they were otherwise isolated, in order to see how much of their behavior could be explained in that way. These eddies are not isolated, however, and eddy-eddy interactions may be an important factor in the eddy propagation. One possibility is that the anticyclonic eddies may be interacting with one another. Two vortices of the same sign, otherwise isolated and with all motion except for the vortex irrotational and inviscid, will tend to rotate about a stationary point between the two [*Kundu*, 1990]. Under the right circumstances in a rotating basin, two vortices of the same rotational sense will merge into one [*Nof and Simon*, 1987]. Cyclonic eddies are also formed at the Big Island, and interactions between the anticyclonic eddies and the cyclonic eddies are also possible, although the cyclonic eddies, unlike the anticyclonic eddies, initially move to the northwest from the Big Island. Vortices of opposite sign in close proximity to one another tend to maintain their distance, with the weaker rotating about the stronger, or moving in parallel lines if they are of similar strength [*Kundu*, 1990]. On a β plane, there is the added tendency for southward and northward meridional motion for anticyclonic and cyclonic eddies, respectively, so the relative position of the eddies is important to consider. All of the above vortex interactions could complicate the propagation of the anticyclonic Big Island eddies, along

with the β plane dynamics and the effect of the mean NEC. Improved altimetric products such as that of *Ducet et al.* [2000], with fine enough resolution to capture the detailed structure of the various vortices and any evolutions as they interact, might allow one to address this possibility in future studies.

This study was initially concerned with determining whether or not the anticyclonic Big Island eddies could account for the sea level variability at Wake Island noted by *Mitchum* [1995]. Of the eight eddies observed in this study, only one (number 2) was tracked to the vicinity of Wake Island. In the tide gauge sea level time series at Wake Island, with the annual cycle removed, there is a peak at the time suggested by the eddy trajectory. This provides some additional validation of the eddy tracking, as with the time series at Johnston Island, discussed previously, but this is only one peak among all the variability of the Wake Island sea level time series. We cannot conclude from the currently available data whether or not the anticyclonic Big Island eddies or energy associated with their decay reach Wake Island, but this question should be reconsidered as better data become available, such as the *Ducet et al.* [2000] mapping. We have found that the eddy propagation is consistent with movement along the $\beta' = 0$ contour, and as Figure 6 shows, this contour does not curve sufficiently northward for the eddies to reach Wake Island if they follow it. In this study, however, β' was computed from the *Levitus et al.* [1994] climatological fields, and it is apparent in Figure 3 that geostrophic velocities computed from this data set can be much slower than instantaneous measurements from such sources as the WOCE surface drifters. The strength, position, and shear of the mean current affect the value of β' . Better estimates of β' and the location of the $\beta' = 0$ contour may be available from the World Ocean Database [*Levitus et al.*, 1998] or from other climatological data sets, and this might allow future studies to address whether or not the hypothesis presented here, that the eddies follow the $\beta' = 0$ contour, is consistent with the Big Island eddies reaching Wake Island.

Acknowledgments. This work was supported by NASA through the Jet Propulsion Laboratory as part of the TOPEX Altimeter Research in Ocean Circulation Mission. Conversations with several people in the Department of Oceanography at the University of Hawaii and in the College of Marine Science at the University of South Florida were very helpful. The paper was also significantly improved by suggestions from two anonymous reviewers.

References

- Chang, P., and S. G. H. Philander, Rossby wave packets in baroclinic mean currents, *Deep Sea Res., Part A*, 36, 17–37, 1989.
- Charney, J. G., and M. E. Stern, On the stability of internal baroclinic jets in a rotating atmosphere, *J. Atmos. Sci.*, 19, 159–172, 1962.
- Ducet, N., P. Y. Le Traon, and G. Reverdin, Global high-resolution mapping of ocean circulation from TOPEX/Poseidon and ERS-1 and -2, *J. Geophys. Res.*, 105, 19,477–19,498, 2000.
- Flierl, G. R., The application of linear quasigeostrophic dynamics to Gulf Stream rings, *J. Phys. Oceanogr.*, 7, 365–379, 1977.
- Flierl, G. R., Rossby wave radiation from a strongly nonlinear warm eddy, *J. Phys. Oceanogr.*, 14, 47–58, 1984.
- Kundu, P. K., *Fluid Mechanics*, 638 pp., Academic, San Diego, Calif., 1990.
- Levitus, S., R. Gelfeld, T. Boyer, and D. Johnson, Results of the NODC and IOC Oceanographic Data Archaeology and Rescue Projects, Key to Oceanographic Records Documentation 19, Natl. Oceanogr. Data Center, Washington, D.C., 1994.
- Levitus, S., T. P. Boyer, M. E. Conkright, T. O'Brien, J. Antonov, C. Stephens, L. Stathoplos, D. Johnson, and R. Gelfeld, *World Ocean Database 1998*, vol. 1, *Introduction*, NOAA Atlas NESDIS 18, Natl. Oceanic and Atmos. Admin., Silver Spring, Md., 1998.
- Lumpkin, C. F., *Eddies and Currents of the Hawaiian Islands*, Ph.D. dissertation, 281 pp., Univ. of Hawaii at Manoa, Honolulu, 1998.
- McWilliams, J. C., and G. R. Flierl, On the evolution of isolated, nonlinear vortices, *J. Phys. Oceanogr.*, 9, 1155–1182, 1979.
- McWilliams, J. C., P. R. Gent, and N. J. Norton, The evolution of balanced, low-mode vortices on the β -plane, *J. Phys. Oceanogr.*, 16, 838–855, 1986.
- Mitchum, G. T., The source of 90-day oscillations at Wake Island, *J. Geophys. Res.*, 100, 2459–2475, 1995.
- Nof, D., and L. M. Simon, Laboratory experiments on the Mergig of nonlinear anticyclonic eddies, *J. Phys. Oceanogr.*, 17, 343–357, 1987.
- Patzert, W. C., Eddies in Hawaiian waters, *Rep. HIG-69-8*, Hawaii Inst. of Geophys., Univ. of Hawaii at Manoa, Honolulu, 1969.
- Seckel, G. R., Seasonal variability and parameterization of the Pacific North Equatorial Current, *Deep Sea Res.*, 22, 379–401, 1975.
- Sutyryn, G. G., and G. R. Flierl, Intense vortex motion on the beta plane: Development of the beta gyres, *J. Atmos. Sci.*, 51, 773–790, 1994.
- Wyrтки, K., Eddies in the Pacific North Equatorial Current, *J. Phys. Oceanogr.*, 12, 746–749, 1982.
- Wyrтки, K., and B. Kilonsky, Mean water and current structure during the Hawaii-to-Tahiti Shuttle Experiment, *J. Phys. Oceanogr.*, 14, 242–254, 1984.

C. L. Holland and G. T. Mitchum, College of Marine Science, University of South Florida, 140 Seventh Avenue South, St. Petersburg, FL 33701. (cholland@marine.usf.edu)

(Received January 14, 2000; revised August 21, 2000; accepted August 31, 2000.)